ResearchGate

See discussions, stats, and author profiles for this publication at: https://www.researchgate.net/publication/275579495

Automated Extraction of Road Markings from Mobile Lidar Point Clouds

Article *in* Photogrammetric Engineering and Remote Sensing · April 2012

DOI: 10.14358/PERS.78.4.331

CITATIONS
129

READS
2,078

4 authors, including:

Bisheng Yang
Wuhan University
160 PUBLICATIONS **3,551** CITATIONS

SEE PROFILE

Qingquan Li
Shenzhen University
400 PUBLICATIONS **8,899** CITATIONS

SEE PROFILE

Jonathan Li
University of Waterloo
531 PUBLICATIONS **8,962** CITATIONS

SEE PROFILE

Some of the authors of this publication are also working on these related projects:

map conflation View project

High Spatial Resolution Imagery Analysis View project

All content following this page was uploaded by Bisheng Yang on 21 June 2015.

The user has requested enhancement of the downloaded file.

Automated Extraction of Road Markings from Mobile Lidar Point Clouds

Bisheng Yang, Lina Fang, Qingquan Li, and Jonathan Li

Abstract

Among implicit information of laser points, the strength of reflection of laser points is closely related to the property of road materials which helps detecting road markings. This paper presents a novel approach to automatically extracting road markings from mobile lidar point clouds. An interpolation method is first used to generate a georeferenced feature image of the point cloud, which helps to isolate the points of road surfaces. Then, an algorithm is used to separate these points within a range according to their strength of reflection. The separated points are further segmented to remove non-road points based on height threshold. Finally, the outlines of road markings are extracted from the segmented points using the semantic knowledge of road markings. The results demonstrated that our method was very promising for automatic extraction of road markings from lidar point clouds collected by a land-based mobile lidar system, an Optech Lynx Mobile Mapper.

Introduction

The car-mounted mobile laser scanning system (mobile lidar) has become a cost-effective solution for capturing spatial data in complex urban areas at the street level quickly and accurately. In particular, mobile lidar can acquire three-dimensional (3D) dense-points, which enable easier building façade reconstruction, man-made object extraction, 3D city modeling, street-scene modeling, and visualization than most other methods. In most cases, the interpretation of 3D lidar point clouds is the first step of the above mentioned tasks.

In recent years, 3D street-scene modeling has shown rapid growth with emerging expansion of location-based services, pedestrian and vehicle navigation, traffic accident, or crime case investigation (Kutterer, 2010). Habib *et al.* (2009) presented a method for classifying terrain points and off-terrain points from lidar data. Clode *et al.* (2010) presented a progressive classification method for separation of road points and non-road points towards automatic detection and vectorization of roads from lidar point clouds. Currently, consumer-grade navigation systems are beginning to move towards presentation of data with 3D models rather than conventional 2D maps. Mobile lidar shows promise for rapid collection of 3D point clouds of the street-scene objects such as building façade, trees, vegetation, traffic signs, poles, and road markings. The above mentioned classification methods are insufficient for classifying car-mounted mobile lidar point clouds (hereafter referred as point clouds) as a great amount of point clouds are located on a vertical plane. Haala *et al.* (2008) and Barber *et al.* (2008) investigated the precision and accuracy of laser scanned point cloud data collected using StreetMapper, a car-mounted mobile lidar system, for urban data capture in different types of urban street scenes and approved that it is operational for urban mapping. An overview of the state of the art mobile mapping systems along with a typical acquisition and processing workflow can be found in Graham (2010). However, compared with advances in hardware systems of mobile lidar, the development of automated algorithms and software tools for the efficient extraction of 3D street-scene objects of interest from point clouds rather lags behind. On the one hand, this is mainly due to huge data volumes and complexity of urban street scenes. On the other hand, efficient methods for interpretation of point clouds are still in the early development stage. Several methods have been proposed for interpreting 3D point clouds and their common steps are the detection of planar or smooth surfaces followed by the classification of points or point clusters based on local point patterns, echo intensity, and echo count information (Vosselman *et al.*, 2004; Darmawati, 2008). Dold and Brenner (2006) presented an automated method for modeling building façades from point clouds. Rutzinger *et al.* (2009) presented a first analysis on the automatic extraction of building walls from point clouds. Their method can separate point clouds according to the hypothesis that the inclination of wall was less than 3°; the segment dimensions were larger than 2 m in height and 0.5 m in width, respectively. Goulette *et al.* (2007) presented a method for automatically extracting the road surface, trees, and vertical surfaces from laser scans. The methods and models that they used were quite simple and the modeled objects lack detail. Hernandez and Marcotegui (2009) presented a method for detection and extraction of artifacts and pavement segmentation from point clouds. First, they generated a range image from point clouds, and then used morphological operators to detect artifacts. Brenner (2009) focused on the automated extraction of poles near road sides for the relative positioning of cars to their environment. Yu *et al.* (2007) studied the use of laser scanners and video cameras in creating detailed models of the road surface (e.g., small cracks on the road surface). Although it is easier to detect road markings from the images, this method requires the co-registration of video camera images and laser scanner points.

Bisheng Yang, Lina Fang, Qingquan Li are with the State Key Laboratory of Information Engineering in Surveying, Mapping and Remote Sensing, Wuhan University, Wuhan, Hubei, China, 430079 (bshyang@whu.edu.cn).

Jonathan Li is with the Department of Geography & Environmental Management, University of Waterloo, Waterloo, Ontario, Canada N2L 3G1.

Photogrammetric Engineering & Remote Sensing
Vol. 78, No. 4, April 2012, pp. 331–338.

0099-1112/12/7804–331/$3.00/0
© 2012 American Society for Photogrammetry and Remote Sensing

Ogawa and Takagi (2006) presented an approach for lane recognition using a vehicle-borne lidar. Their method identified lanes with curvature, yaw angles, and offsets using the Hough transform. Moreover, an extended Kalman filter was adopted for tracking the discontinuous lane marks in the region of interest. Soheilian *et al.* (2010) presented an automatic approach to road marking reconstruction using stereo pairs acquired by a mobile mapping system in a dense urban area. Edge points were extracted from the left and right images of a stereo pair. The known geometric specifications of road marking objects were used to constrain the recognition of strips. Smadja *et al.* (2010) focused on road environment interpretation from a mobile mapping system. The lane mark detection algorithms were implemented based on edge-based image processing. The morphological opening operator was used to remove the objects thinner than the specified size of lane marks. Zhang (2010) presented a method of identifying road regions and road edges using mobile lidar range data. The road segments and road-edge points were detected according to a local extreme-signal detection filter according to elevation data with a prior knowledge of the minimal width of roads. Finally, road-edges and curbs of the road segments were further validated using curb detection by projecting the data to the ground plane. Chen *et al.* (2009) presented a method that mainly used point clouds along with laser intensity images for detecting traffic signs and lane markings. Prior knowledge (e.g., time stamp, scanning angle) was incorporated for lane marking detection using the Hough transform.

According to the literature, challenges still exist in automated interpretation of point clouds. It is evident that the methods for point interpretation depend on the objectives of applications and the geometric characteristics of objects. Patterns or shapes play an important role for the point interpretation and are helpful for extracting man-made objects from range images and point clouds. Structure- or pattern-based object extraction has received a great deal of attention in recent years. Pu and Vosselman (2009) proposed a method for automatically extracting windows from point clouds. Their method was able to model windows as holes, triangulate the point clouds, and finally define large triangles as windows.

Generally, road markings show a set of predefined shapes. Hence, these predefined shapes can easily be modeled as many structures (e.g., rectangle, dotted lines). Our aim is to automatically extract road markings from mobile lidar point clouds. In this paper, first we propose a method for generating a georeferenced feature image (hereafter referred to as feature image) from mobile lidar point clouds. Next, we present a solution for extracting the approximate outline of road surface from the generated georeferenced feature images. The point clouds that fall in the extracted outline are further filtered according to the reflectance intensities of point clouds, and then a georeferenced reflectance intensity image is generated according to the intensities of the point clouds. Second, we present a technique for extracting road markings from such a georeferenced reflectance intensity image according to the structures of the predefined shapes. Finally, two datasets were selected to evaluate the effectiveness of our method and conclusions are drawn at the end of this paper.

Mobile Lidar Point Cloud Segmentation

Generation of Feature Imagery

This section describes how a georeferenced feature image was generated from point clouds. First, the mobile lidar points were projected onto the XOY plane. A rectangle box can easily be determined by the coordinates of the bottom-left and top-right corners of the feature image. The width and height of the feature image can be calculated by:

$$\begin{cases} W = (X_{max} - X_{min})/GSD \\ H = (Y_{max} - Y_{min})/GSD \end{cases} \tag{1}$$

where W and H are the width and height of the feature image, respectively, (X_{min}, Y_{min}) and (X_{max}, Y_{max}) are the coordinates of the bottom-left and top-right corners of the feature image, respectively, and GSD (ground sample distance) is the spatial resolution. Once the width and height of the feature image are determined, the laser points can be located in each cell of the feature image with calculated grey values.

The spatial distribution of laser points implies the local geometric features of street-scene objects. Hence, the grey values of the feature image should reflect the spatial distribution of laser points. The grey value of each cell of the feature image is determined by the Inverse Distance Weighted (IDW) interpolation method that is widely used for interpolation of digital elevation models (DEM). As the points in each cell are not 2.5D but 3D in the feature images here, the weight associated with each point should be carefully determined in order to reflect the spatial distribution pattern. To fulfill the above requirement, we define the following rules to determine the weight associated with each point:

Rule 1: The larger weight should be assigned to the higher point.

Rule 2: The larger weight should be assigned to the point closer to the center.

These two rules indicate that the weight of each point is determined by two factors, namely, planar distance and height difference. Once the weight of each point is determined, the grey value of each cell is calculated as follows by the IDW interpolation method:

$$F_{ij} = \left(\sum_{k=1}^{n_{ij}} W_{ijk} \cdot Z_{ijk}\right) \Big/ \left(\sum_{k=1}^{n_{ij}} W_{ijk}\right) \tag{2}$$

where

$$W_{ijk} = \alpha \cdot W_{ijk}^{XY} + \beta \cdot W_{ijk}^{H} \tag{3}$$

$$\begin{cases} W_{ijk}^{XY} = \sqrt{2} \cdot GSD/D_{ij}^{k} \\ W_{ijk}^{H} = H_{ij}^{k} \cdot (h_{min(ij)} - Z_{min})/(Z_{max} - h_{max(ij)}) \\ \alpha + \beta = 1.0 \end{cases} \tag{4}$$

where α and β are the coefficients of weights,

$$D_{ij}^{k} = \sqrt{(x_{ij}^{k} - x_{0}^{ij})^2 + (y_{ij}^{k} - y_{0}^{ij})^2} \tag{5}$$

where n_{ij} is the number of scanning points in the cell (i, j), $h_{min(ij)}$ and $h_{max(ij)}$ are the lowest and highest elevations in the cell (i, j), respectively, Z_{max} and Z_{min} are the lowest and highest elevations in the whole scanning area, respectively, (x_0^{ij}, y_0^{ij}) is the coordinate of the center of the cell (i, j), D_{ij}^{k} is the distance between point(x_{ij}^{k}, y_{ij}^{k}) and (x_0^{ij}, y_0^{ij}), α, and β are the coefficients of weights that need tuned.

Equation 5 demonstrates that the grey value of each cell of the georeferenced feature image is determined by the planar distance values between the points and the center of cell and the height differences between the points and the lowest height point of the cell. Hence, a georeferenced feature image is generated with the specified values of α and β. The generated georeferenced feature image will be used for segmentation of mobile lidar point clouds.

Segmentation of Road Point Cloud

As mentioned above, the larger grey values were assigned to the higher points when the feature image was generated.

(a) (b)

Figure 1. Segmentation results of the feature image: (a) Original point clouds, and (b) Extraction of the point clouds within outline of road in georeferenced image.

Hence, buildings and trees have larger grey values over their surrounding areas (e.g., roads). A grey-value threshold can be specified to filter the areas of larger grey values according to the histogram analysis on the feature image. In this study, the discrete discriminant analysis (Goldstein and Dillon, 1978) method was applied to automatically specify the threshold because of its robustness. First, we used this method to find the maximum and minimum grey values of the feature image, respectively. Then, we calculated the between-cluster variances under an assumed threshold. Finally, we determined the optimal threshold that has the largest value of the between-cluster variances and used this optimal threshold to classify the cells into different categories. According to this solution, the points located on the outline of the road surfaces can easily be extracted from the point clouds. Figure 1 illustrates the segmentation results of the feature image.

Once the points located on the outlines of road surfaces are extracted, the pedestrians and cars can easily be eliminated from the extracted road points according to the height threshold. Hence, the points on the road surfaces can be extracted successfully. Generally speaking, the laser scanners usually also record the strength of the reflected laser pulse. This property can be used to distinguish road markings from the road surfaces (Vosselman, 2009). The test datasets used in this study were collected by Optech Lynx Mobile Mapper, and the reflectance values of point clouds were classified according to the material types of objects. Table 1 lists the reflectance values of different objects in the datasets collected by the Optech Lynx Mobile Mapper system.

In order to extract the point clouds of road markings, a two-step filter operator was applied. The first step is to extract the point clouds within the reflectance intensity value range of 100 to 300 from the point clouds extracted. The second step is to further remove those points (e.g., cars, pedestrian) that have a higher elevation compared with those of the neighborhood points associated. Figure 2 illustrates an example. Figure 2a shows the point clouds of road and neighborhood associated. It can be seen from Figure 2c that the point clouds of road marking were well maintained although there are a few noisy points. Hence, a viable solution should be implemented to extract road markings from the point clouds after the two-step filter operator.

TABLE 1. THE REFLECTANCE VALUES OF DIFFERENT OBJECTS

Reflectance value	Material types	Potential objects
1 to 100	Asphalt, Concrete Pavement	Road, Bridge
100 to 300	Painted layer	Road marking, Curbstone
300+	Vegetation	Bush, Grass

Extraction of Road Markings

In most cases, road markings show linear features and have dimensions of known width and length. Figure 3 illustrates an example.

On the one hand, the shapes and arrangement of road markings provides semantic knowledge for the extraction of road markings. On the other hand, the prior semantic knowledge of road marking should be incorporated for extracting the road markings, particularly for extracting those occluded or in incomplete shapes. To extract road markings from the point clouds filtered by the two-step filter operator, a georeferenced reflectance intensity image was firstly generated according to the method mentioned earlier. Then, the 4-connected regions of the georeferenced intensity image were labeled for detecting the regions of road markings as illustrated in Figure 4.

For each 4-connected region, a set of parameters, namely, the area of each 4-connected region, the area, length, and width of the minimum bounding box of each 4-connected region, and the ellipse with the same second-moments as the 4-connected region were calculated, respectively. Then, these criterions were calculated by.

$$e = \frac{\sqrt{a^2 + b^2}}{a} \tag{6}$$

$$ratio = S_1/S_2$$

where a and b are the long and short axis of ellipse, S_1 and S_2 are the areas of 4-connected region and the minimum bounding box of it associated, e is the scalar that specifies the eccentricity of the ellipse that has the same second-moments as the 4-connected region. The value of e is between 0 and 1.0. Suppose that the value of e is 0.0. The 4-connected region is a circle; *ratio* is the degree of filling of

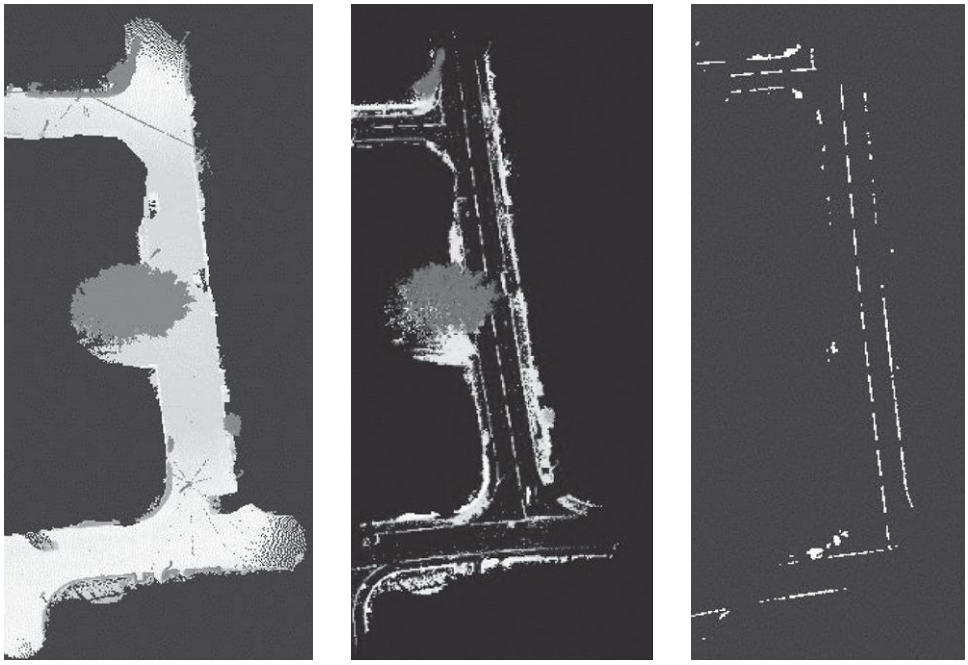

(a) (b) (c)

Figure 2. Segmentation of the point clouds of a road: (a) Original point clouds, (b) filtered result by reflectance intensity, and (c) filtered result by height.

(a) (b)

Figure 3. Two types of shapes and arrangement of road markings.

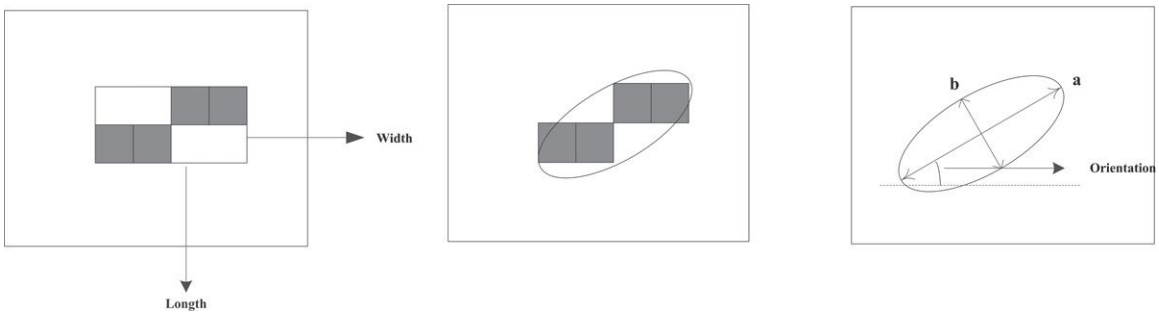

Figure 4. Labeled 4-connected regions of georeferenced reflectance intensity image.

4-conneted. It is an important indicator to measure whether the 4-connected region is a regular region. The value of ratio is also between 0 and 1. Suppose the ratio is 1.0. The 4-connected region is a regular rectangle.

In order to extract the regions of road markings from the georeferenced reflectance intensity image, the corresponding thresholds can be specified to *e* and *ratio* according to the resolution of the georeferenced reflectance intensity image and the size and shape of road markings. Figure 5 shows a result of 4-connected regions extraction.

It can be seen that the other regions of irregular shapes were well filtered from the georeferenced reflectance intensity image by labeling 4-connected regions. As we aimed to extract the road markings of linear shapes, a progressive

(a) (b)

Figure 5. Extracted 4-connected region from the georeferenced reflectance intensity.

probabilistic Hough Transformation (PPHT) operator (Matas *et al.*, 2000) was applied to extract the linear features (dashed mark lines) from the georeferenced reflectance intensity image filtered. The Hough transform is a popular method for identifying lines. The original Hough transform is a linear transformation, which is relatively fast in searching for a binary image of straight lines.

The progressive probabilistic Hough transform (PPHT) is a variation of the standard Hough transform that computes an extent for individual lines in addition to the orientation. It is "probabilistic" because, rather than accumulating every possible point in the accumulator plane, it accumulates only a fraction of them. The PPHT minimizes the computation time needed to detect lines by exploiting the difference in the fraction of votes needed to reliably detect lines with different numbers of supporting points (Matas *et al.*, 2000). Hence, a PPHT operator was selected to extract dashed mark lines from the georeferenced reflectance intensity image after filtering. Once the minimum length of line segment extracted is given, the line segments can be extracted from the georeferenced reflectance intensity image filtered and vectorized. Within the algorithm of PPHT, the parameters of *threshold*, *param*1 and *param*2 are taken into account. The *threshold* is the value in the accumulator plane that must be reached for the routine to report a line. The *param*1 specifies the minimum length of a line segment that will be returned. The *param*2 specifies the separation between collinear segments required for the algorithm not to join them into a single longer segment. Figure 6 shows a result of linear features detected by the PPHT operator.

Figure 6. Lines detected by a PPHT operator and vectorization.

Results and Discussion

The 3D point clouds used in this study were captured by an Optech Lynx Mobile Mapper system, which consists of two Optech laser scanners, one GPS receiver, and an Applanix inertial measuring unit (IMU), which collects lidar data at more than 100,000 measurements per second with a 360° field of view (FOV). The point clouds of two sites were selected for assessing the performance of the proposed method (see Figure 7).

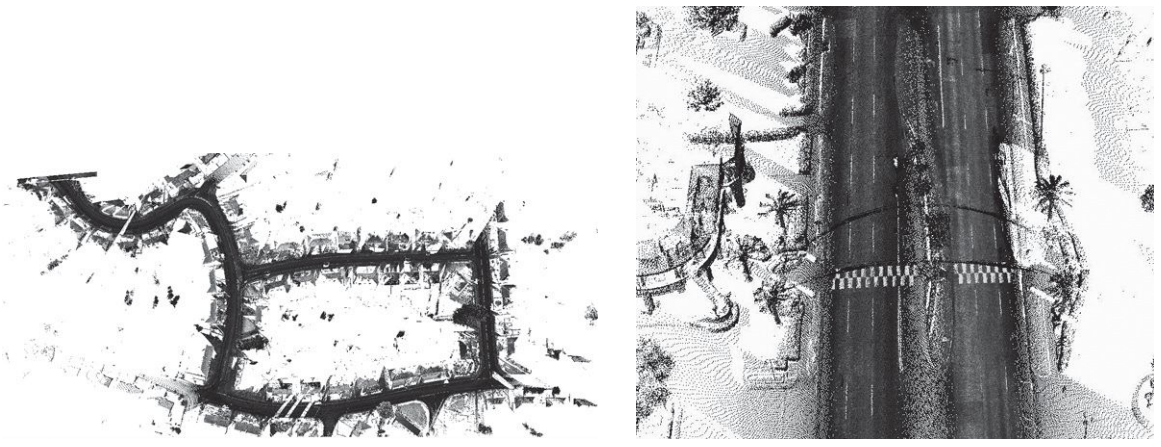

(a) (b)

Figure 7. An overview of the tested sites: (a) a residential area, and (b) part of an urban area with roads consisting of multiple lanes.

The first test site shown in Figure 7a is a residential area with dimensions of 400 m $\times$ 350 m. It contains vegetation (e.g., trees, bushes), buildings, power lines, and moving objects (e.g., pedestrians and cars). The second test site shown in Figure 7b is part of an urban area with roads consisting of multiple lanes.

The georeferenced feature image of mobile lidar point clouds was first generated. In our study, the georeferenced feature images were generated with a resolution of 0.2 m based on the sizes of road markings. Figure 8 illustrates the georeferenced feature images of the two datasets.
To extract the approximate outlines of road, the method of discrete discriminant analysis (Goldstein and Dillon, 1978) was adopted to extract the point clouds located on the outlines of road. Then, the point clouds of road surfaces were further filtered according to the reflectance values of points and height. Finally, a georeferenced reflectance intensity image of road markings was generated. Figure 9 illustrates the georeferenced reflectance intensity images of two test sites.

We specified the parameters of *e* and *ratio* as 0.95 and 0.8, respectively, for labeling 4-connected regions of the georeferenced reflectance intensity image and removing those regions of irregular shapes. The values of *e* and *ratio* are 0.95 and 0.8, respectively, which means that extracted regions are approximately rectangles. Figure 10 illustrates the results of labeling 4-connected regions. It is easy to see that most of the regions of irregular shapes were eliminated from the georeferenced reflectance intensity images.

Once the georeferenced reflectance intensity image was labeled by 4-connected regions, those regions of irregular shapes were removed as shown in Figure 10. According to the final step of the proposed method, the PPHT operator was adopted to extract the road marking from the georeferenced reflectance intensity images after 4-connected regions were labeled. In the PPHT operator, the *threshold*, *param*1, and

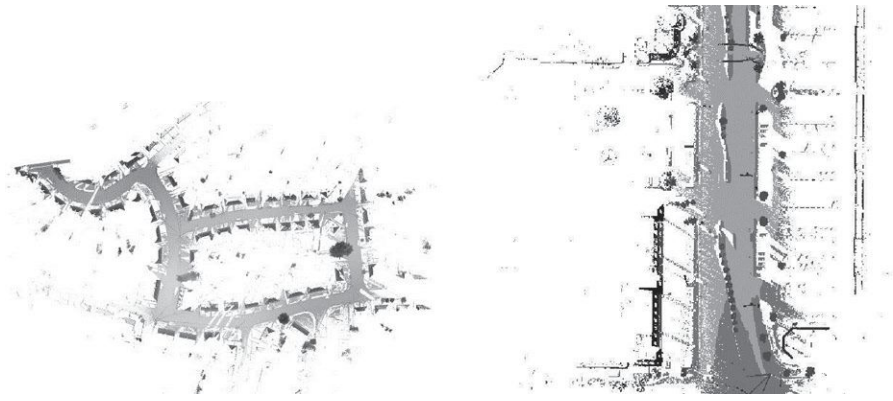

(a) (b)

Figure 8. Generated georeferenced feature images: (a) a residential area, and (b) a downtown area.

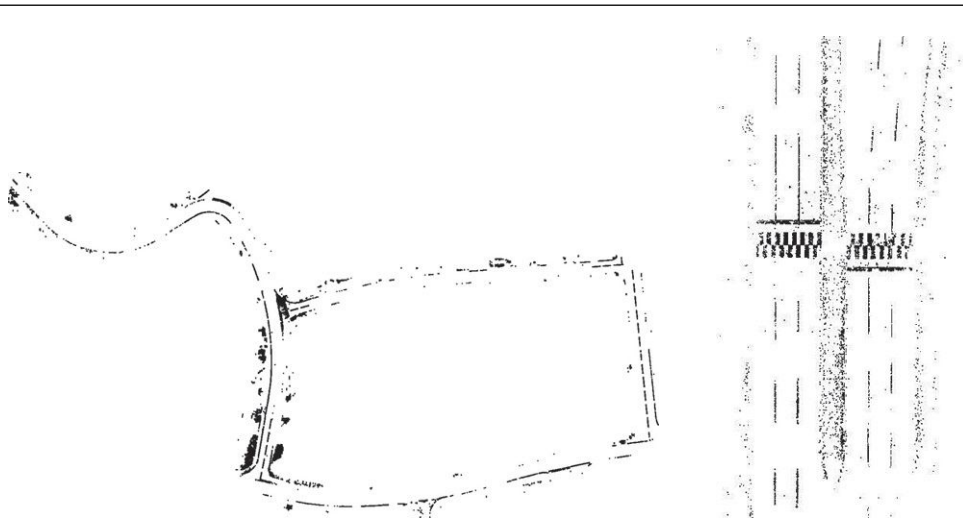

(a) (b)

Figure 9. Generated georeferenced reflectance intensity image of road markings: (a) a residential area, and (b) a downtown area.

*param*2 are set as 50, 30,10, respectively, to achieve better results of road marking extraction. The extracted segments were further tuned based on the linear least-squares fitting for vectorization. Figure 11 shows the extracted road markings.

Compared with the scenes of the two datasets, the point clouds of the residential area contain different types of objects (e.g., cars, poles, buildings), where some road markings were partly or fully occluded. The urban area is complicated and contains multiple lanes. Although the point clouds of the residential area contain various objects, the proposed method still extracted a good result of road markings. The extracted results of road markings demonstrate that the proposed method shows a good performance for extracting road markings from mobile lidar point clouds.

Conclusions

In this paper, we have proposed a method for extracting road markings from mobile lidar point clouds. The proposed method first generates a georeferenced feature image of point clouds followed by extracting the approximate outline of road using discrete discriminant analysis from the georeferenced feature image. Second, the proposed method further segments the point clouds of road according to the reflectance strength of point clouds for extracting the point

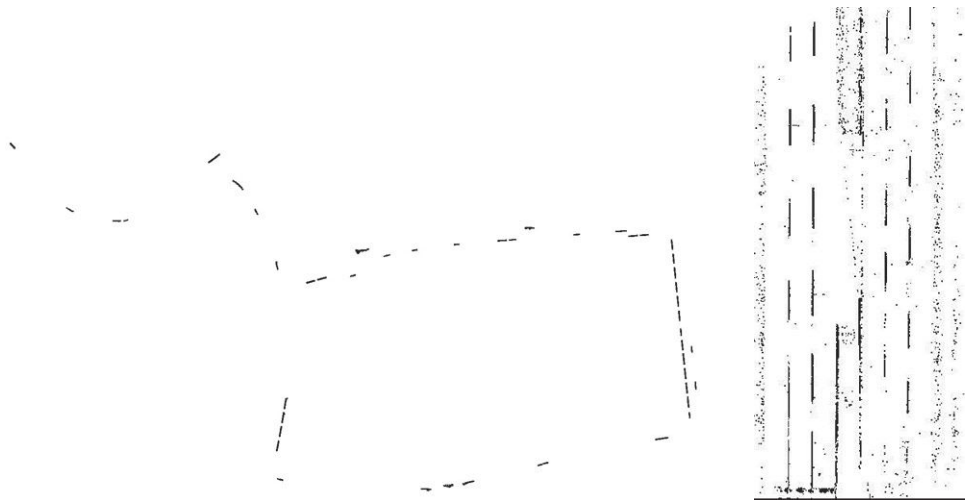

Figure 10. Results of labeling 4-connected regions of scenes (a) and (b) in Figure 9.

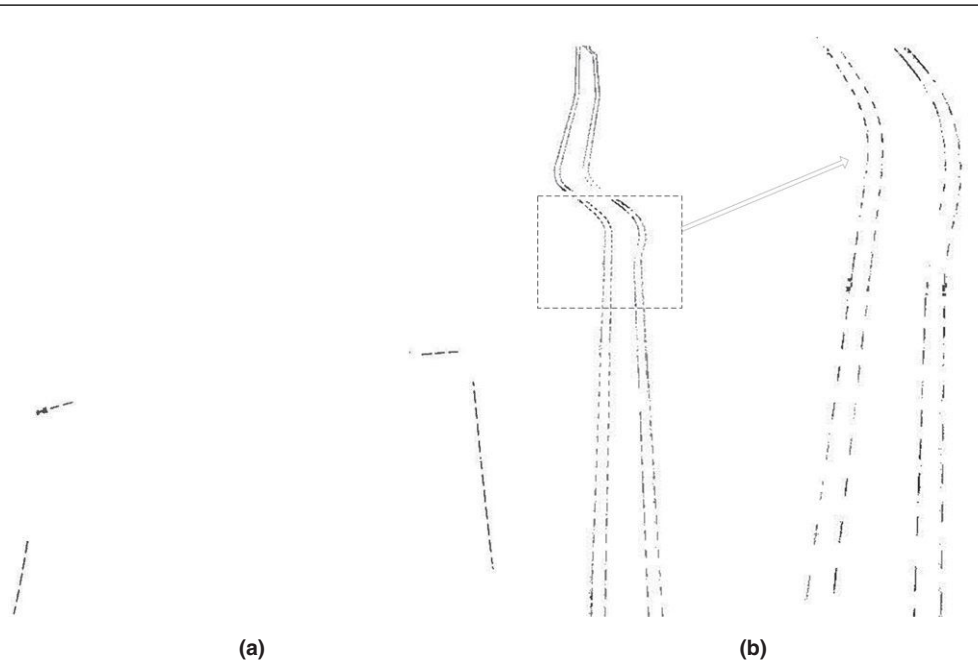

Figure 11. Extracted road markings: (a) a residential area, and (b) a downtown area.

clouds of road markings. Finally, the proposed method generates a georeferenced reflectance strength image of the point clouds of road markings, labeling the regions of road markings according to the shape and arrangement of road markings, and applies the PPHT operator for extracting road markings. In order to improve the performance of road markings extraction, the proposed method incorporates the semantic knowledge (e.g., shape, pattern) of road markings, which is particularly helpful for extracting those road markings occluded or with incomplete shapes. The above key steps were successfully integrated into the proposed method.

Two different datasets were selected for checking the validity of the proposed method. The experimental results demonstrated that the proposed method shows a good performance for extracting road marking from mobile lidar point clouds. Moreover, the match between the extracted road markings and the original point clouds proves that the proposed method detects and extracts road markings correctly. In addition, the proposed method converts the semantic knowledge of road markings, namely, size, shape, and arrangement, into two parameters (*e* and *ratio*) for labeling the regions of road markings from the georeferenced reflectance intensity image. The two parameters can easily be tuned according to size, shape, and arrangement of road markings, which was proven to be quite beneficial for extracting road markings that have partially diminished. The extracted road markings can easily be modeled for 3D road network in detail. Further studies are needed for more elaborate and complex road markings for example, at road intersections.

Acknowledgments

The work presented in this paper was substantially supported by NSFC (No.41071268), the State Key Laboratory of Resources and Environmental Information Systems, CAS of China (No. 2010KF0001SA), the outstanding talented project from the Ministry of Education of P. R. China (NCET-07-0643), and the Fundamental Research Funds for the Central Universities (No. 3103005). The LYNX Mobile Mapper datasets were provided by Optech, Inc.

References

Barber, D., J. Mills, and V.S. Smith, 2008. Geometric validation of a ground-based mobile laser scanning system, *ISPRS Journal of Photogrammetry and Remote Sensing*, 63(1):128–141.

Brenner, C., 2009. Extraction of features from mobile laser scanning data for future driver assistance systems, *Advances in GIScience*, *Lecture Notes in Geoinformation and Cartography* (M. Sester, L. Bernard, and V. Paelke, editors), Springer, pp. 25–42.

Chen, X., M. Stroila, R. Wang, B. Kohlmeyer, N. Alwar, and J. Bach, 2009. Next generation map marking: Georeferenced ground-level LiDAR point clouds for automatic retro-reflective road feature extraction, *Proceedings of the 17th ACM SIGSPATIAL International Conference on Advances in Geographic Information Systems,* Seattle, Washington, unpaginated CD-ROM, 7 p.

Clode, S., F. Rottensteiner, P. Kootsookos, and E. Zelniker, 2007. Detection and vectorization of roads from lidar data, *Photogrammetric Engineering & Remote Sensing*, 73(5):517–535.

Darmawati, A., 2008. *Utilization of Multiple Echo Information for Classification of Airborne Laser Scanning Data*, Master's Thesis, International Institute for Geo-Information Science and Earth Observation (ITC), Enschede, The Netherlands.

Dold, C., and C. Brenner, 2006. Registration of terrestrial laser scanning data using planar patches and image data, *International Archives of Photogrammetry and Remote Sensing*, Dresden, Germany, 25-27 September, 36(5):25–27.

Goldstein, M., and W. R. Dillon, 1978. *Discrete Discriminant Analysis*, John Wiley and Sons, New York, 186 p.

Graham, L., 2010. Mobile mapping system overview, *Photogrammetric Engineering & Remote Sensing,* 76(3):222–229.

Haala, N., M. Peter, A. Cefalu, and J. Kremer, 2008. Mobile lidar mapping for urban data capture, *Proceedings of the 14th International Conference on Virtual Systems and Multimedia*, 20-25 October, Limassol Cyprus, pp. 95–100.

Habib, A.F., Y.-C. Chang, and D.C. Lee, 2009.Occlusion-based methodology for the classification of lidar data, *Photogrammetric Engineering & Remote Sensing*, 75(6):703–713.

Hernandez, J., and B. Marcotegui, 2009. Filtering of artifacts and pavement segmentation from mobile lidar data, *Proceedings of the ISPRS Workshop*, 01-02 September, Paris, France, unpaginated CD-ROM.

Kutterer, H., 2010. *Mobile Mapping, Airborne and Terrestrial Laser Scanning* (G. Vosselman and H.-G. Mass, editors), Whittles Publishing/CRC Press, Caithness, UK, pp. 293–311.

Matas, J., C. Galambos, and J. Kitter, 2000. Robust detection of lines using the progressive probabilistic Hough transform, *Vision and Image Understanding*, 78(1):119–137.

Ogawa. T., and K. Takagi, 2006. Lane recognition using on-vehicle LiDAR, *Proceedings of IEEE Intelligent Vehicles Symposium*, 13–15 June, Tokyo, Japan, pp. 845–848.

Pu, S., and G. Vosselman, 2009. Knowledge based reconstruction of building models from terrestrial laser scanning data, *ISPRS Journal of Photogrammetry and Remote Sensing*, 64(6):575–584.

Rutzinger, M., F. Rottensteiner, and N. Pfeifer, 2009. A comparison of evaluation techniques for building extraction from airborne laser scanning, *IEEE Journal of Selected Topics in Applied Earth Observations and Remote Sensing*, 2(1):11–20.

Smadja. L., J. Ninot, and T. Gavrilovic. 2010. Global environment interpretation from a new mobile mapping system, *Proceedings of IEEE Intelligent Vehicles Symposium*, 21-24 June, San Diego, California, pp. 941–948.

Soheilian, B., N. Paparoditis, and D. Boldo, 2010. 3D road marking reconstruction from street-level calibrated stereo pairs, *ISPRS Journal of Photogrammetry and Remote Sensing*, 65(5):347–359.

Vosselman, G., B.G.H. Gorte, G. Sithole, and T. Rabbani, 2004. Recognising structure in laser scanner point clouds, *International Archives of Photogrammetry, Remote Sensing and Spatial Information Sciences*, 04-06 October, Freiburg, Germany, 6(8/W2):33–38.

Yu, S.J., S.R. Sukumar, A.F. Koschan, D.L. Page, and M.A. Abidi, 2007. 3D reconstruction of road surfaces using an integrated multi-sensory approach, *Optics and Lasers in Engineering*, 45(7):808–818.

Zhang, W., 2010. LiDAR-based road and road edge detection, *Proceedings of IEEE Intelligent Vehicles Symposium,* San Diego, California, 21-24 June, pp. 845–848.

View publication stats